

## Bioelectric, tissue, and molecular characteristics of the gastric mucosa at different times of ischemia

Peña-Mercado Eduardo<sup>1</sup> , Garcia-Lorenzana Mario<sup>2</sup>, Patiño-Morales Carlos César<sup>3</sup>, Montecillo-Aguado Mayra<sup>4</sup>, Huerta-Yepez Sara<sup>5</sup> and Beltran Nohra E<sup>6</sup> 

<sup>1</sup>Posgrado en Ciencias Naturales e Ingeniería, Unidad Cuajimalpa, Universidad Autónoma Metropolitana, CDMX 05340, Mexico;

<sup>2</sup>Departamento de Biología de la Reproducción, Unidad Iztapalapa, Universidad Autónoma Metropolitana, CDMX 09340, Mexico;

<sup>3</sup>Laboratorio de Investigación en Biología del Desarrollo y Teratogénesis Experimental, Hospital Infantil de México, Federico Gómez, CDMX 06720, Mexico; <sup>4</sup>Doctorado en Ciencias Biológicas, Facultad de Medicina, Universidad Nacional Autónoma de México, CDMX 04510, Mexico; <sup>5</sup>Unidad de Investigación en Enfermedades Hematológicas, Hospital Infantil de México, Federico Gómez, CDMX 06720, Mexico; <sup>6</sup>Departamento de Procesos y Tecnología, Unidad Cuajimalpa, Universidad Autónoma Metropolitana, CDMX 05340, Mexico

Corresponding author: Beltran Nohra E. Email: nbeltran@cua.uam.mx

### Impact statement

Delay in the diagnosis of shock, as well as its treatment, can generate alterations that can lead to death in patients in critical condition. In this work, thresholds of impedance parameters are proposed, and the expression of markers of inflammatory process and apoptosis is analyzed to identify the time of ischemia at which the gastric mucosa loses its barrier function. Increases in  $R_L$  and  $X_H$  ( $>87 \Omega$  and  $>13.5 -j\Omega$ , respectively) in addition to the expression of iNOS, TNF $\alpha$ , COX-2, and apoptotic biomarkers suggest that damage to the gastric mucosa generated up to 60 min of ischemia may be reversible; and with proper treatment in this period of time, the extent of the lesion could be minimized, or the regeneration process accelerated after the reperfusion stage, preserving the barrier function of the gastric mucosa.

### Abstract

Gastrointestinal ischemia may be presented as a complication associated with late shock detection in patients in critical condition. Prolonged ischemia can cause mucosal integrity to lose its barrier function, triggering alterations that can induce organ dysfunction and lead to death. Electrical impedance spectroscopy has been proposed to identify early alteration in ischemia-induced gastric mucosa in this type of patients. This work analyzed changes in impedance parameters, and tissue and molecular alterations that allow us to identify the time of ischemia in which the gastric mucosa still maintains its barrier function. The animals were randomly distributed in four groups: Control, Ischemia 60, 90, and 120 min. Impedance parameters were measured and predictive values were determined to categorize the degree of injury using a receiver operating characteristic curve. Markers of inflammatory process and apoptosis (iNOS, TNF $\alpha$ , COX-2, and Caspase-3) were analyzed. The largest increase in impedance parameters occurred in the ischemia 90 and 120 min groups, with resistance at low frequencies ( $R_L$ ) and reactance at high frequencies ( $X_H$ ) being the most related to damage, allowing prediction of the occurrence of reversible and irreversible tissue damage. Histological analysis and apoptosis assay showed progressive mucosal

deterioration with irreversible damage ( $p < 0.001$ ) starting from 90 min of ischemia. Furthermore, a significant increase in the expression of iNOS, TNF $\alpha$ , and COX-2 was identified in addition to apoptosis in the gastric mucosa starting from 90 min of ischemia. Tissue damage generated by an ischemia time greater than 60 min induces loss of barrier function in the gastric mucosa.

**Keywords:** Gastric ischemia, electrical impedance spectroscopy, gastric impedance parameters, digital pathology, bioimpedance, biomarkers

*Experimental Biology and Medicine* 2021; 246: 1968–1980. DOI: 10.1177/15353702211021601

## Introduction

Shock refers to a life-threatening circulatory failure caused by an imbalance between supply and demand of cellular oxygen. In patients in critical condition, vital signs, clotting tests, and hematopoietic procedures are monitored to identify it. However, there are difficulties in diagnosing it since the physiological changes that occur are subtle.<sup>1</sup> This is because in the body, compensation mechanisms are activated through which blood is redistributed to vital organs, generating gastrointestinal ischemia induced by vasoconstriction in the splanchnic circulation.<sup>2</sup>

Shock can be difficult to identify accurately, and it may be hard to treat due to the multitude of options available,<sup>3</sup> however, delayed detection of signs associated with hemodynamic engagement in the body, delayed treatment,<sup>4</sup> and the treatment itself, can precipitate the development of an injury in the gastrointestinal tract.<sup>5</sup> As a result, bacteria and toxic mediators released from the injured mucosa can be transported through the circulation and mesenteric lymph nodes, increasing the chance of sepsis,<sup>2</sup> and cause multiple organ dysfunction, which is directly related to morbidity and mortality in patients in critical condition.<sup>6</sup>

At the clinical level, the presence of complications that promote the formation of gastric ulcers has been identified, specifically in gastric ischemia; medical treatment includes fluid resuscitation and the placement of a nasogastric aspiration tube.<sup>7</sup> To identify early alterations in the gastric mucosa and microcirculation changes generated by hypoperfusion in patients in critical condition, gastric tonometry and capnometry have been used, with certain limitations.<sup>8</sup> Electrical impedance spectroscopy (EIS) is the study of the passive electrical properties of biological tissue (at the cellular and molecular level) at different frequencies. Impedance is the total effect of two separate orthogonal dimensions: electrical resistance (R) that restricts electron flow and dissipates energy, and electrical reactance (X) which is the ability of membranes to store and release energy.<sup>9</sup> The EIS offers various clinical applications. It has been used to detect potentially malignant oral lesions,<sup>10</sup> as well as to determine mucosal integrity in patients with gastroesophageal reflux.<sup>11</sup> In addition, it allows measuring and monitoring of fluid accumulation in patients with acute decompensated heart failure,<sup>12</sup> and evaluation hydration status in dialyzed patients with chronic kidney disease.<sup>13</sup>

The EIS allows tissues to be characterized and serves to identify the progression of tissue damage induced by ischemic conditions. Under oxygen deprivation conditions, cell edema is one of the early effects that can be identified by this technique. If the critical duration is exceeded, which varies depending on the type of organ or cell, alterations occur at the membrane level that induce death, so the degree of injury is determined by the magnitude and duration of ischemia.<sup>14,15</sup> Disturbances in intra and extracellular volume, as well as alterations in cell membrane integrity, directly affect R and X, respectively. Recently, EIS has also been used to identify brain injuries induced by Ischemia/Reperfusion (I/R)<sup>16</sup> and to characterize different types of cell death.<sup>17</sup>

Our research group has used EIS to monitor and detect early alterations in gastric mucosa associated with ischemia in patients in critical condition and in animal models.<sup>9,18</sup> In addition, we proposed a tissue lesion index (TLI) in the gastric mucosa, based on the quantification of variables related to I/R injury<sup>19</sup> that can be directly related to changes in gastric impedance. The variables considered were the vascular area, glandular lumen area, the number of damaged cells (edema, apoptosis, or necrosis), and the depth of epithelial erosion zones, and from these parameters, a characterization was made as to the presence of tissue damage, based on a score  $>3$ .<sup>20</sup>

Nitric oxide synthase (NOS) is a family of enzymes that use oxygen and nitrogen (derived from the amino acid arginine) to catalyze nitric oxide (NO) production. Inducible nitric oxide synthase (iNOS) is a calcium-independent enzyme, which is expressed during the inflammatory process and during hypoxic conditions. The increase in the production of NO under reperfusion conditions has been closely linked to an increase in tissue damage in affected tissues.<sup>21,22</sup> Tumor necrosis factor alpha (TNF $\alpha$ ) is a cytokine produced mainly by macrophages. This cytokine plays a key role in pathological conditions such as infections, injuries, inflammation, and tumor development. Once released by macrophages, it activates other immune cells and mediates the production of other pro-inflammatory cytokines.<sup>23</sup> In addition, it has been reported that the increase in the expression of hypoxia induced TNF $\alpha$  increases the permeability of intestinal epithelial cells<sup>24</sup> and the respiratory tract *in vitro*, facilitating the diffusion of bacterial antigens and toxins that can cause inflammation.<sup>25</sup> Cyclooxygenase-2 (COX-2) is an inducible enzyme predominantly during inflammation, so it is regulated by pro-inflammatory agents, including cytokines and endotoxins. There is evidence of an increased COX-2 expression during gastrointestinal I/R conditions.<sup>26,27</sup>

Due to the gastrointestinal complications associated with the diagnosis and treatment of shock, it is important to identify alteration in tissues that may suggest that damage to the ischemic gastric mucosa is still reversible and has not lost its barrier function. In this work, changes in impedance parameters were analyzed, along with tissue and molecular alterations, that may make it possible to identify the time of ischemia in which the gastric mucosa still maintains its barrier function.

## Materials and methods

### Animal preparation and ethical considerations

Thirty-two male Wistar rats (250–300 g) were used, raised in the vivarium of the Universidad Autonoma Metropolitana - Iztapalapa, which remained under a controlled environment ( $22^{\circ}\text{C} \pm 2^{\circ}\text{C}$ ; 50%–60% relative humidity and 12 h–12 h light–dark cycles) with access to food and water *ad libitum* until the time of surgery. The rats were randomly distributed in four experimental groups: Control, Ischemia (Isc) 60, 90 and 120 min. The experimental protocol was approved by the Ethics Committee of the Centro Nacional de Investigacion en Imagenologia e

Instrumentacion Medica, under the Official Mexican Standard (NOM-062-ZOO-1999).

### Surgical procedure

The rats were anesthetized with a mixture of xylazine and ketamine (10–90 mg/kg) administered intraperitoneally, and kept with isoflurane inhaled at 2% until the experiments were completed. Gastric mucosal damage from ischemia was done by occlusion of the celiac artery.<sup>28</sup> The rats underwent a midline laparotomy, the artery was identified and occluded with a clamp to block blood flow for the corresponding time for each of the groups. In the Control group, the surgical procedure was performed without inducing ischemia. After the corresponding time, a sagittal gastrotomy was performed on the major curvature, the gastric lumen was washed with saline solution and an impedance spectroscopy probe and nasogastric tube (ISP/NGT) was introduced to perform impedance measurements; consecutively, biopsies of the glandular portion were taken. Biopsies for histological analysis were fixed in a stabilized neutral formalin solution (10%), while those for molecular analysis were stored at  $-80^{\circ}\text{C}$  until processing. At the end of the experiments, the animals were euthanized in accordance with NOM-033-ZOO-1995.

### Measurements of gastric impedance

Impedance spectra were obtained through an ISP/NGT, which has four silver electrodes at its distal end. An alternating electric current of 1 mA was injected into the gastric mucosa through the external electrodes, and several measurements were performed for each animal at 23 frequencies (215 Hz to 1 MHz), with software designed specifically for the spectrometer. The device measured the tissue voltage and calculated impedance parameters for resistance and reactance. Gastric mucosa spectra have two dispersion zones, one at frequencies below 10 kHz (Low frequencies) and the other above 10 kHz (High frequencies). The spectra were processed offline using a mathematical model to calculate the characteristic parameters of the gastric mucosa: central resistance at low ( $R_L$ ) and high ( $R_H$ ) frequencies, and central reactance at low ( $X_L$ ) and high ( $X_H$ ) frequencies.<sup>29</sup>

### Qualitative and quantitative histological analysis

Biopsies were dehydrated with gradual ethanol, processed, and embedded in paraffin into a tissue microarray. Nine cross-sections and nine longitudinal cuts were made 3  $\mu\text{m}$  thick with a semi-automatic rotation microtome (RM2245, LEICA), and were then stained with Hematoxylin-Eosin (H&E). To evaluate mucus production, cross-sections were made 3  $\mu\text{m}$  thick which were stained with Periodic acid-Schiff–Alcian blue (PAS-AB). The cuts were scanned and digitized (Aperio CS2, Leica Biosystems) for qualitative and quantitative analysis through digital pathology. The manufacturer's algorithm was used for the analysis of the expression of each of the markers. Briefly, the algorithms included in the Aperio CS2 equipment provide us with a series of quantitative measurements, including intensity, concentration, and percentage of positive

staining. To calculate the degree of injury in gastric mucosa, a TLI proposed by Peña-Mercado *et al.*<sup>20</sup> was used, which is related to changes in gastric impedance parameters to identify the maximum sensitivity and specificity value from a curve of the operating characteristics of the receiver (ROC).

### Immunohistochemistry

The section tissues were deparaffinized and subjected to antigenic recovery in sodium citrate buffer (pH 6). Endogenous peroxidase blockage was performed with methanol and hydrogen peroxide (3%) for 30 min. The blocking of non-specific binding was done for 3 h. The section tissues were incubated with the primary anti-iNOS (Rabbit polyclonal, Santa Cruz Biotechnology, SC-649; 1:200), anti-TNF $\alpha$  (Polyclonal Goat, SC-1351, 1:200), and anti-COX-2 (Polyclonal Rabbit, Novus, NB-100-689) antibodies in a wet chamber at room temperature throughout the night. For negative control, an isotype control (Calbiochem millipore, NI01-100 (rabbit; NI02-100 (goat)) was used. They were then incubated with the secondary antibody conjugated to horseradish peroxidase (HRP) (anti-rabbit: MP-7401, anti-goat: MP-7405; Vector Laboratories) for 30 min inside the wet chamber at room temperature. The antigen-antibody complex was revealed with an immunodetection kit (Vector Laboratories) and the counterstain was done with Hematoxylin. The immunostaining tissues were scanned and digitized (Aperio CS2, Leica Biosystems) to quantify the intensity of staining (Intensity/area).

### Western blot

Biopsies were homogenized to extract total proteins with the T-PER Tissue Protein Extraction Reagent (Thermo Scientific, #7850) lysis buffer with protease inhibitor (EDTA-free Protease Inhibitor Cocktail, 11873580001, Sigma-Aldrich) added. The concentration of proteins was determined by the direct microvolume method using the NanoDrop™ Lite (Thermo Scientific™) spectrometer. Sixty micrograms of total protein per sample were separated into a 10% acrylamide gel (SDS/PAGE) and transferred into a nitrocellulose membrane (Bio-Rad, Hercules). The membranes were incubated with primary antibody anti-Caspase-3 (SC-56053; 1:1000) and anti-GAPDH (SC-48167, 1:10,000) in blocking solution overnight at 4°C. Subsequently, they were rinsed and incubated with secondary antibody coupled to HRP (SC-516102) diluted 1:1000 in blocking solution for 2 h. Immunodetection was done by chemiluminescence (Super Signal® West Femto, Thermo Scientific). Densitometry analysis was performed with Image J software, version 1.45 (National Institute of Health).

### Apoptosis assay (TUNEL)

Detection of DNA fragmentation was performed using the TUNEL (Terminal dUTP nick-end labeling) technique with the *In situ* cell death detection fluorescein kit (Roche Diagnostics). Longitudinal slices were made 5  $\mu\text{m}$  thick,

which were pre-assembled into electrocharged slides (Superfrost Plus Glass Slides, Electron Microscopy Sciences). The tissue sections were deparaffinized and subjected to antigenic recovery in sodium citrate buffer (20× Immuno/DNA Retriever with Citrate) for 40 min in a retriever for antigen unmasking (Retriever 2100, Electron Microscopy Sciences); they were then incubated with the mixture of TUNEL reaction conjugated to fluorescein for 60 min at room temperature in a wet chamber in complete darkness. The tissue sections were mounted with Fluoroshield™ with DAPI (Sigma-Aldrich). The number of reactive nuclei was quantified in three randomly selected fields (×400) of the upper portion of the gastric mucosa in three slices per specimen.

### Statistical analysis

The data were analyzed using IBM SPSS 21 (IBM Corporation) and GraphPad Prism 9 (GraphPad Software). Parametric data were analyzed with an ANOVA test followed by a post hoc Tukey test. For non-parametric data, a Kruskal Wallis test was performed followed by a post hoc T3 Dunnett test. To determine the optimal value of impedance parameters ( $R_L$ ,  $R_H$ ,  $X_L$ ,  $X_H$ ) in which damage to the gastric mucosa can be predicted, an ROC curve was performed, considering the score of the  $TLI > 3$  as true positives (tissue injury). To identify which impedance parameter has the greatest relationship to gastric mucosal damage (TLI), a segmented linear regression was made by taking as a “breakpoint” the predictive value (PV) with greater sensitivity and specificity of each

parameter. Data are presented as mean  $\pm$  SEM. The value of  $p < 0.01$  was considered statistically significant.

## Results

### Analysis of gastric impedance parameters

To identify the effect of different ischemia times on the gastric mucosa of rodents, impedance spectra (resistance and reactance) were obtained (Figure 1(a)). A Cole–Cole plot (resistance vs reactance) was made (Figure 1(b)) and gastric impedance parameters of experimental groups were calculated at low and high frequencies. In the impedance spectra, an increase was identified in the  $R_L$  and  $X_L$  (frequencies  $< 10,000$  Hz) in the ischemic groups, with group Isc 90 min having the greatest change. Meanwhile, at frequencies greater than  $10,000$  Hz, no major changes in the  $R_H$  of ischemic groups were observed; however,  $X_L$  and  $X_H$  in the groups Isc 90 and Isc 120 min had a greater increase than in the group Isc 60 min (Figure 1(a)). The Cole–Cole plot identified the two dispersion zones at low and high frequencies and showed a right shift as tissue damage associated with different ischemia times increases, with greater changes in the Isc 90 and Isc 120 min groups (Figure 1(b)).

$R_L$ ,  $R_H$ ,  $X_L$  and  $X_H$  of the Isc 60 min, Isc 90 min, and Isc 120 min groups had a significant increase ( $p < 0.001$ ) with respect to the Control group (Figure 1(c) to (f), respectively). The biggest changes between ischemia groups occurred in reactance. Significant differences in  $R_L$ ,  $X_L$  and  $X_H$  ( $p < 0.001$ ) were observed between the Isc 60 min vs Isc 90

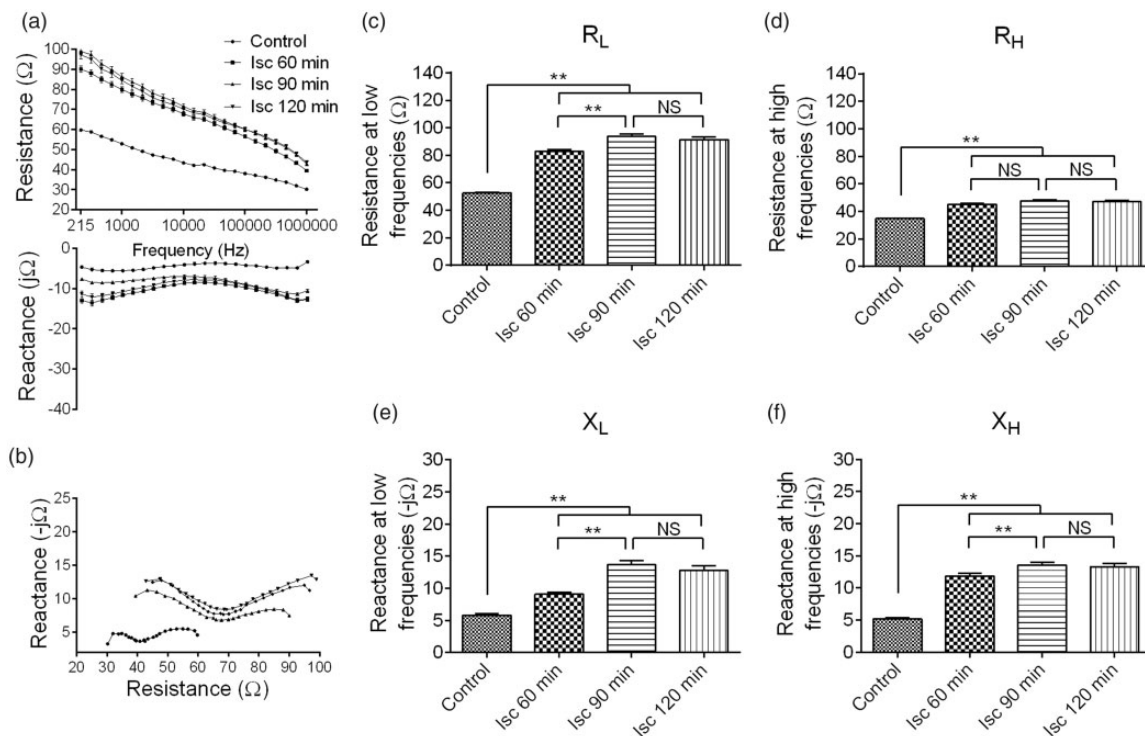


**Figure 1.** (a) Gastric impedance spectra (resistance and reactance) of the Control, Isc 60, 90, and 120 min groups. (b) Cole–Cole plot (resistance vs reactance). (c) to (f) Graphical representation of measurements of impedance parameters of the Control group and experimental groups. (c) Resistance at low frequencies ( $R_L$ ). (d) Resistance at high frequencies ( $R_H$ ). (e) Reactance at low frequencies ( $X_L$ ). (f) Reactance at high frequencies ( $X_H$ ). Data are expressed as the mean  $\pm$  SEM. \*\*  $p < 0.001$ ; NS: not significant.

groups. In the Isc 120 min group, it was observed that impedance parameters tend to decrease; however, this was not significant with respect to the Isc 90 min group (Table 1).

### Histopathological analysis of damage in the gastric mucosa

The epithelium, the area of the lamina propria, and blood vessels were observed in the histopathological analysis of

the Control group, without apparent data of injury; glandular architecture was found preserved (Figure 2(a) and (e)). In the Isc 60 min group, cells in the process of necrosis and others with hydropic degeneration were identified, as well as significant vascular congestion from the upper portion to the fundus of the gastric gland (Figure 2(b) and (f)). In the Isc 90 min group, there was an identification of epithelial cells that detached from the basement membrane (anoikis) to the gastric lumen, areas of bleeding and

**Table 1.** Relation of gastric impedance parameters with the score of the tissue lesion index, expression of iNOS, TNF $\alpha$ , COX-2, cleaved Caspase-3, and the TUNEL apoptosis assay under conditions: Control and Ischemia for 60, 90, and 120 min.

	Control	Isc 60 min	Isc 90 min	Isc 120 min
R <sub>L</sub> ( $\Omega$ )	52.57 $\pm$ 1.70	82.75 $\pm$ 1.37	93.74 $\pm$ 1.82	91.41 $\pm$ 2.07
R <sub>H</sub> ( $\Omega$ )	34.80 $\pm$ 0.36	45.25 $\pm$ 0.61	47.46 $\pm$ 0.73	47.14 $\pm$ 0.93
X <sub>L</sub> (-j $\Omega$ )	5.77 $\pm$ 0.27	9.09 $\pm$ 0.26	13.69 $\pm$ 0.62	12.80 $\pm$ 0.71
X <sub>H</sub> (-j $\Omega$ )	5.17 $\pm$ 0.18	11.88 $\pm$ 0.40	13.57 $\pm$ 0.47	13.32 $\pm$ 0.55
TLI	0.82 $\pm$ 0.15	3.86 $\pm$ 0.10	4.76 $\pm$ 0.07	5.34 $\pm$ 0.12
iNOS (Int/ $\mu$ m <sup>2</sup> )	722.3 $\pm$ 83.20	1664 $\pm$ 283.4	5642 $\pm$ 608.7	5557 $\pm$ 330.5
TNF $\alpha$ (Int/ $\mu$ m <sup>2</sup> )	653.3 $\pm$ 38.08	545.9 $\pm$ 112	2492 $\pm$ 463.5	2565 $\pm$ 180.4
COX-2 (Int/ $\mu$ m <sup>2</sup> )	2452 $\pm$ 285.2	4940 $\pm$ 390.8	6564 $\pm$ 506	5436 $\pm$ 323.8
Cleaved Caspase-3 (AU)	0	0	0.44 $\pm$ 0.07	1.67 $\pm$ 0.28
TUNEL (positive cells)	2.57 $\pm$ 0.53	23.37 $\pm$ 2.19	61.52 $\pm$ 3.81	64.0 $\pm$ 7.08

Data are expressed as the mean  $\pm$  SEM.

R<sub>L</sub>: resistance at low frequencies; R<sub>H</sub>: resistance at high frequencies; X<sub>L</sub>: reactance at low frequencies; X<sub>H</sub>: reactance at high frequencies; TLI: tissue lesion index; AU: arbitrary units.

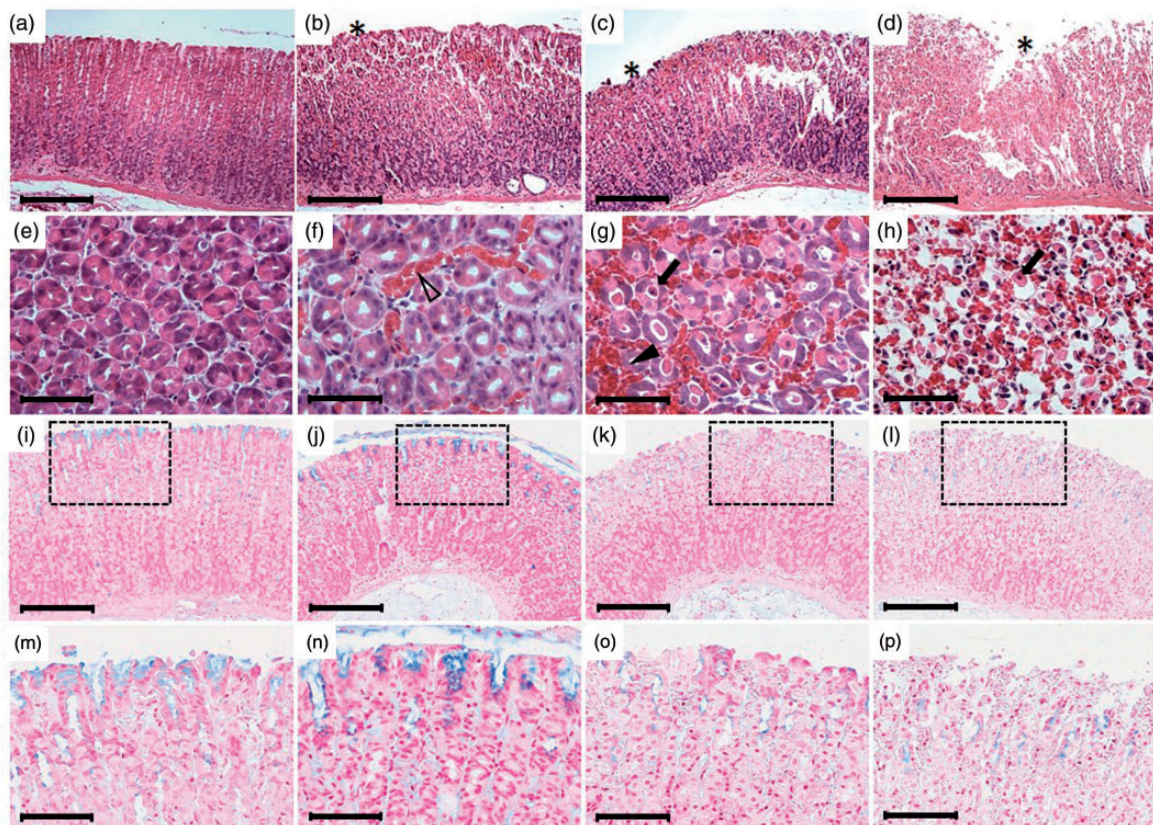


**Figure 2.** Photomicrography of longitudinal and cross slices of rat gastric mucosa dyed with H&E. Groups: Control (a) and (e), Isc 60 min (b) and (f), Isc 90 min (c) and (g), and Isc 120 min (d) and (h). PAS-AB. Groups: Control (e, i), Isc 60 min (f, j), Isc 90 min (g, k), and Isc 120 min (h, l). Identifiers: (\*) areas of surface exfoliation and erosion in the gastric mucosa (hollow arrowhead) vascular congestion, (black arrowhead) hemorrhage, (black arrow) cell in apoptosis, (dotted area) surface mucous cells. (a to d, i to l) Scale bar: 200  $\mu$ m; (e to h) Scale bar: 100  $\mu$ m. (m to p) Scale bar: 80  $\mu$ m. (A color version of this figure is available in the online journal.)

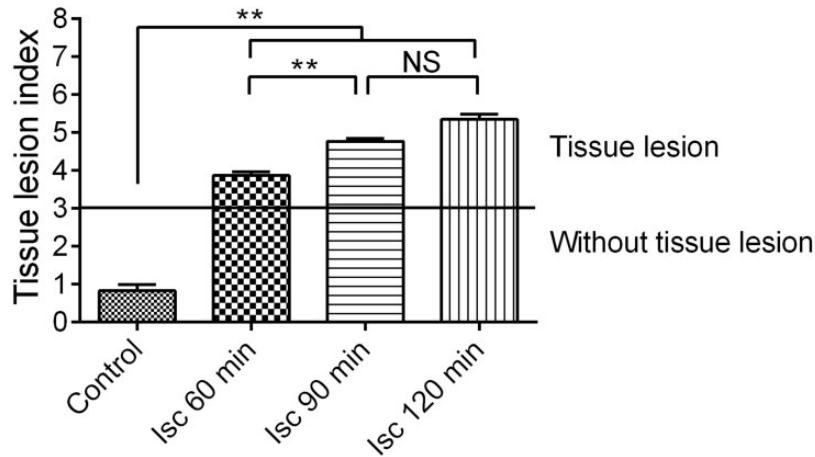


**Figure 3.** Graphical representation of the TLI score of the Control group vs experimental groups. Data are expressed as the mean  $\pm$  SEM. \*\* $p < 0.001$ ; NS: not significant.

vascular congestion, as well as flaking of surface epithelium cells and loss of glandular architecture in some areas of the oxyntic portion of the mucosa (Figure 2(c) and (g)). In the Isc 120 min group, there was widespread detachment of glandular epithelium cells in the surface portion with major bleeding, and areas of ulceration were identified (Figure 2 (d) and (h)).

On the other hand, the staining of PAS-AB (Figure 2(i) to (p)) showed surface mucous cells of the gastric mucosa with intense alcianophilia (blue color). In addition, PAS-positive cells (bright magenta color) were identified in the neck and basal portion of gastric gland pit in the Control group (Figure 2(i) and (m)), which is maintained in the Isc 60 min group (Figure 2(j) and (n)), while in the Isc 90 (Figure 2(k) and (o)) and Isc 120 min groups (Figure 2(l) and (p)) the staining affinity was lost along the surface epithelium and glandular epithelium of the gastric mucosa indicating that the production of acidic and neutral glycosaminoglycans is lost, respectively.

According to histological analysis carried out with both stains, morphological alterations associated with irreversible damage were evident, as well as the decrease in the production of acidic and neutral glycosaminoglycans, which compromises the first protective barrier of the epithelium of the gastric mucosa subjected to ischemia times starting from 90 min.

### Quantitative analysis of damage in the gastric mucosa

A significant increase ( $p < 0.001$ ) was observed in the TLI score in ischemic groups with respect to the Control group. Isc 60, 90 and 120 min groups presented a score  $>3$  and according to the categorization of the TLI, there is tissue injury; however, the severity increases in a time-dependent manner, with the Isc 120 min group showing greater damage. Even so, starting from the 90 min of ischemia, the functional integrity of the gastric mucosa can be compromised (Figure 3).

### Relationship between gastric impedance parameters and the TLI

Taken together, the results described in Table 1 showed that all impedance parameters had an increase that relates to morphological changes quantified with the TLI, with  $R_L$  and  $X_H$  showing the largest changes between the Control group and ischemia groups. Moreover, the  $X_L$  showed an abrupt increase in the Isc 60 min group compared to the Isc 90 min group.

### ROC curve to categorize the degree of injury

With the data obtained from the analysis of each of the gastric impedance parameters and the TLI score, an ROC curve was derived to predict the damage to the gastric mucosa generated by prolonged ischemia. The result of the ROC curve identified that  $R_L$  and  $X_H$  were the parameters with the highest area under the curve (AUC); however, the AUC of the  $X_L$  and the  $X_H$  are very similar (Table 2). The result of segmented linear regression was consistent with the AUC, with  $R_L$  and  $X_H$  being the impedance parameters that best relate ( $r^2 = 0.72$  and  $r^2 = 0.66$ , respectively) to gastric mucosal damage (TLI) induced by a long-term ischemia model.

According to the ROC curve estimation, the PV for  $R_L$  and  $X_H$  was  $79 \Omega$  and  $10.5 -j\Omega$ , respectively. However, to identify the time of ischemia in which damage to the gastric mucosa can still be reversible, other values were selected to separate the true negatives (TN-no injury) and positives (TP-with injury). For  $R_L$  the values for identifying TN and TP were  $70 \Omega$  and  $87 \Omega$ , respectively, while the values for the  $X_H$  were  $7.7 -j\Omega$  and  $13.5 -j\Omega$ , respectively (Table 2). According to these results, values found within the range of TN and TP may present data of early inflammatory process and reversible cell damage, which do not compromise the barrier function of the gastric mucosa.

### Immunostaining of biomarkers of inflammatory processes and apoptosis

The immunohistochemical analysis of iNOS showed mild cytoplasmic immunoreactivity in epithelial cells of the gastric mucosa in the Isc 60 min group (Figures 4(b) and 5(b)),

**Table 2.** Analysis of the ROC curve of gastric impedance parameters.

	AUC	TN	Se-Sp	PV	Se-Sp	TP	Sp-Se
$R_L$ ( $\Omega$ )	$0.86 \pm 0.022^{+O\&}$	70	0.90–0.60	79	0.78–0.78	87	0.90–0.60
$R_H$ ( $\Omega$ )	$0.78 \pm 0.028^{*\&}$	38	0.90–0.43	43	0.71–0.71	48.7	0.90–0.40
$X_L$ ( $-j\Omega$ )	$0.81 \pm 0.023^*$	5.4	0.90–0.27	9	0.75–0.75	10.5	0.90–0.65
$X_H$ ( $-j\Omega$ )	$0.82 \pm 0.025^{**}$	7.7	0.90–0.52	10.5	0.74–0.74	13.5	0.90–0.50

\* $p < 0.001$ ;  $R_L$  vs  $R_H$ ,  $X_L$ ,  $X_H$ ;  $^+p < 0.001$ ;  $R_H$  vs  $R_L$ ,  $X_L$ ,  $X_H$ ;  $^Op < 0.001$ ;  $X_L$  vs  $R_L$ ,  $R_H$ ,  $X_H$ ;  $^{\&}p < 0.001$ ;  $X_H$  vs  $R_L$ ,  $R_H$ ,  $X_L$ .

ROC: receiver operating characteristic curve;  $R_L$ : resistance at low frequencies;  $R_H$ : resistance at high frequencies;  $X_L$ : reactance at low frequencies;  $X_H$ : reactance at high frequencies; AUC: area under the curve; TN: true negatives; TP: true positives; PV: predictive value; Se: sensitivity; Sp: specificity.

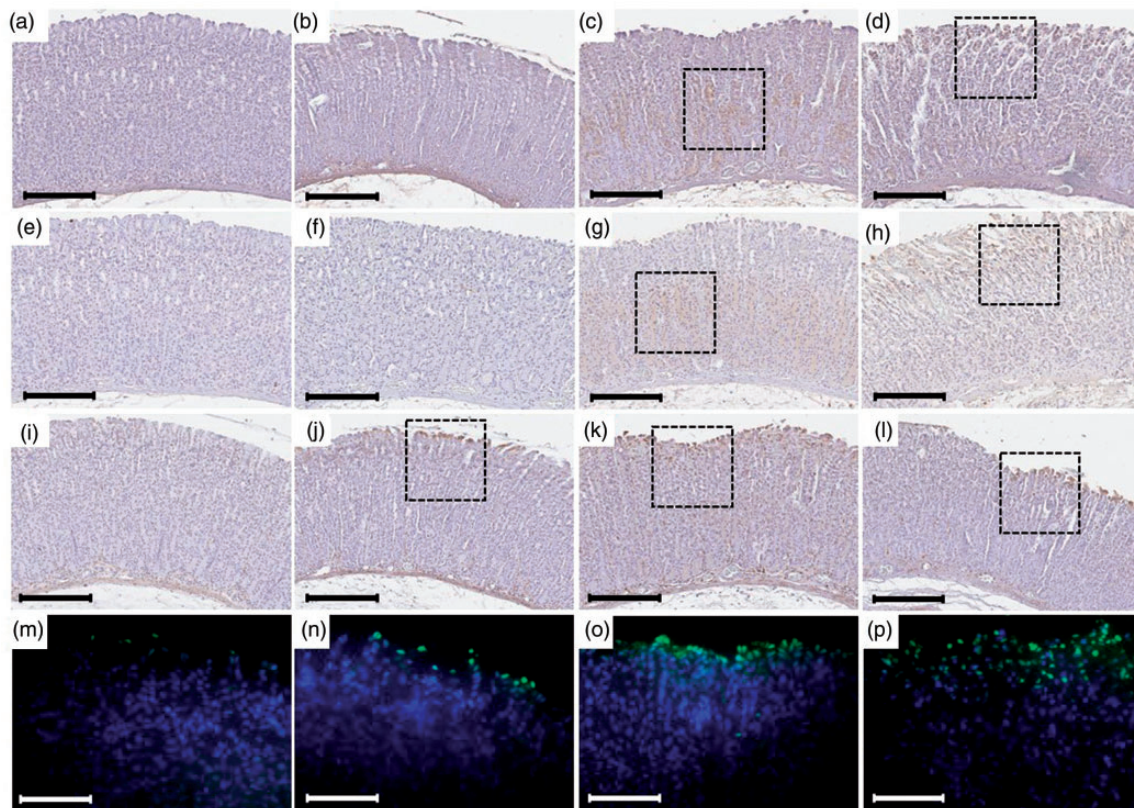


**Figure 4.** Representative photomicrography of immunostaining of iNOS: (a) Control, (b) Isc 60 min, (c) Isc 90 min, and (d) Isc 120 min. Immunostaining of TNF $\alpha$ : (e) Control, (f) Isc 60 min, (g) Isc 90 min, and (h) Isc 120 min. Immunostaining of COX-2: (i) Control, (j) Isc 60 min, (k) Isc 90 min, and (l) Isc 120 min. Identifiers: (dotted area) area of the highest expression. Scale bar: 200  $\mu$ m. Detection of DNA fragmentation by TUNEL apoptosis assay (Terminal dUTP Nick-End Labeling) in experimental groups: (m) Control, (n) Isc 60 min, (o) Isc 90 min and (p) Isc 120 min. Scale bar: 100  $\mu$ m. (A color version of this figure is available in the online journal.)

which increased significantly ( $p < 0.001$ ) in the Isc 90 and Isc 120 min groups (Figures 4(c), (d) and 5(c), (d)), with the Isc 90 min group having the maximum peak of expression (Figure 6(a)). Immunostaining of TNF $\alpha$  showed no changes in expression between the Control group and the Isc 60 min group (Figures 4(e), (f) and 5(e), (f)), while in the Isc 90 and Isc 120 min groups (Figures 4(g), (h) and 5(g), (h)) the level of expression increased significantly ( $p < 0.001$ ), with the Isc 90 min group having the highest level of expression (Figure 6(b)).

Immunohistochemical testing for COX-2 detection showed positive immunoreactivity in some cell types of the muscularis mucosae (Figure 4(i)) and the lamina propria (Figure 5(i)) in the Control group. Under ischemic conditions, a significant increase ( $p < 0.01$ ) in the expression of COX-2 was observed in endothelial and surface epithelium

cells in the Isc 60 (Figures 4(j) and 5(j)) and Isc 90 min (Figures 4(k) and 5(k)) groups. In the Isc 120 min group (Figures 4(l) and 5(l)), a decrease in the expression of COX-2 was identified with respect to the Isc 90 min group (Figure 6(c)), probably associated with the degradation of tissue in the upper portion of the gastric mucosa.

DNA fragmentation of damaged epithelial cells was analyzed using the apoptosis assay (TUNEL) which identified some positive TUNEL cells in the surface epithelium in the Control group (Figure 4(m)). In ischemic groups (Figure 4(n) to (p)), a significant increase ( $p < 0.001$ ) was observed in the number of positive cells and therefore in the depth of the mucosa, with the groups of 90 and 120 min (Figure 6(d)) of ischemia having the greatest increase. After 120 min of ischemia, the depth of the apoptotic area reaches the oxyntic portion of the mucosa.

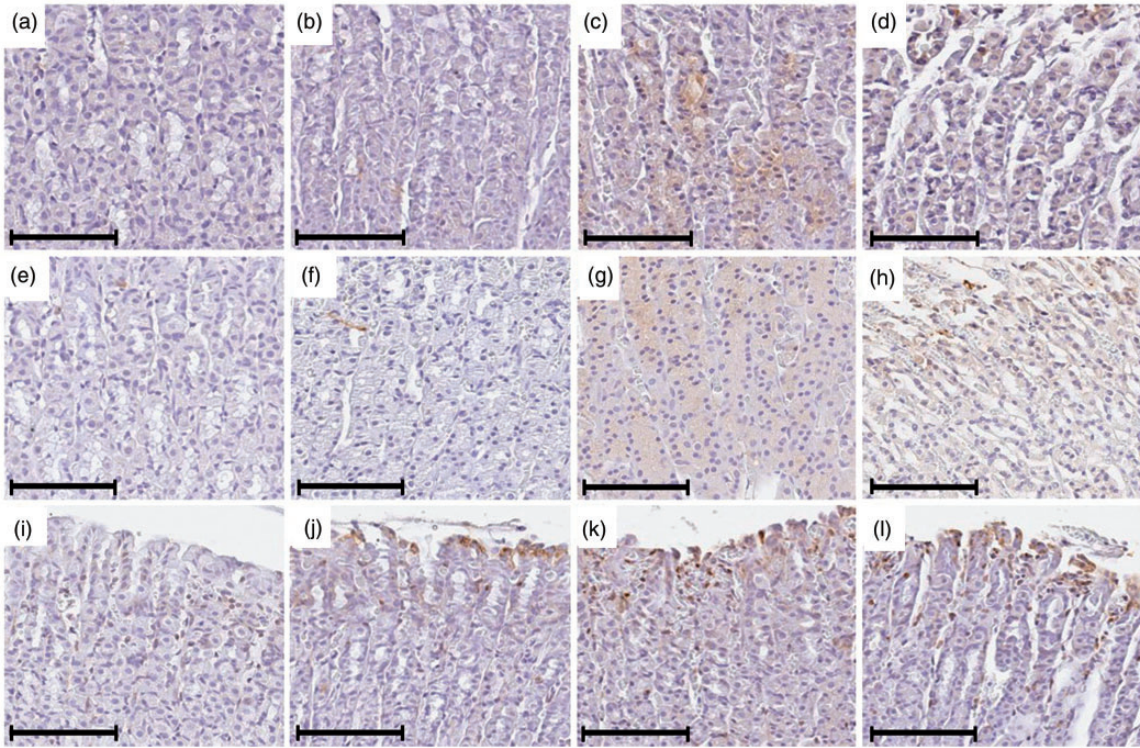


**Figure 5.** Representative photomicrography of immunostaining of iNOS: (a) Control, (b) Isc 60 min, (c) Isc 90 min, and (d) Isc 120 min. Immunostaining of TNF $\alpha$ : (e) Control, (f) Isc 60 min, (g) Isc 90 min, and (h) Isc 120 min. Immunostaining of COX-2: (i) Control, (j) Isc 60 min, (k) Isc 90 min, and (l) Isc 120 min. Scale bar: 80  $\mu$ m. (A color version of this figure is available in the online journal.)

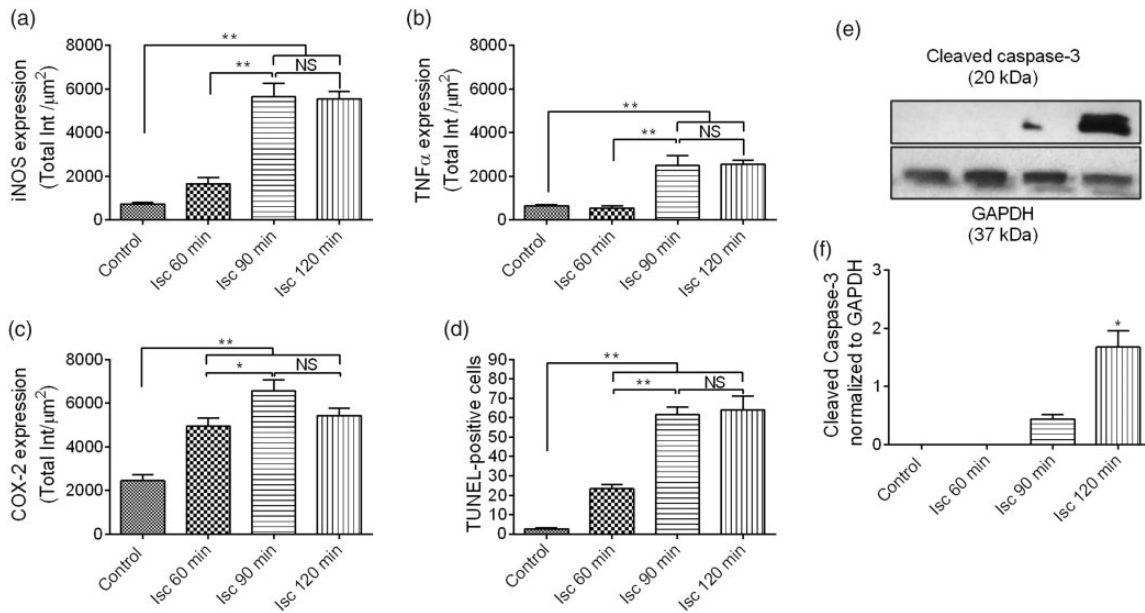


**Figure 6.** Graphical representation of the expression of iNOS (a), TNF $\alpha$  (b), COX-2 (c), and TUNEL apoptosis assay (d). Immunodetection and quantitative analysis of cleaved caspase-3 (e) and (f). The experiments were performed in triplicate and the data are expressed as the mean  $\pm$  SEM. \* $p$  < 0.01, \*\* $p$  < 0.001; NS: not significant.

The immunodetection analysis of Caspase-3 by Western blot (Figure 6(e) and (f)) showed a gradual increase in the expression of active caspase-3 starting from the Isc 90 min group, with the Isc 120 min group being the one with the highest level of expression ( $p$  < 0.01), while in the Control

group and Isc 60 min group, cleaved Caspase-3 was not identified.

Finally, with the results obtained, a scatter plot was made to compare the expression of iNOS, TNF $\alpha$ , COX-2 vs the thresholds of the impedance parameters vs the TLI

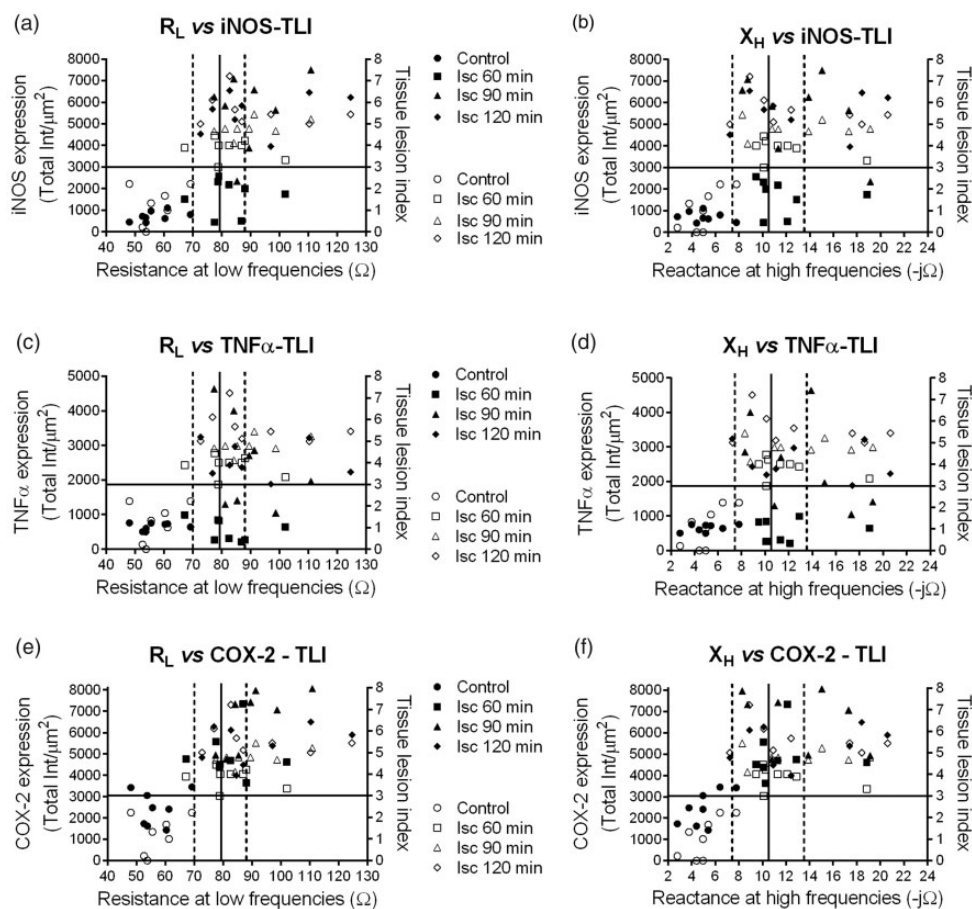


**Figure 7.** Comparison of gastric impedance parameters vs the expression of iNOS, TNF $\alpha$ , and COX-2 vs TLI. (a, c, e) Resistance at low frequencies ( $R_L$ ); (b, d, f) Reactance at high frequencies ( $X_H$ ). Black symbols correspond to the expression values of iNOS, TNF $\alpha$ , and COX-2. The hollow symbols correspond to the values of the TLI.

score (Figure 7(a) to (f)). The graph showed that the expression of iNOS in the subjects of the Control group and Isc 60 min group (87.5%) is found below a score of 3 of the TLI and TP-with injury of impedance parameters, while Isc 90 and 120 min groups are distributed in the zone of inflammatory process (TN-TP) and irreversible damage (TP-with injury) (Figure 7(a) and (b)). The expression of TNF $\alpha$  in the subjects of the Control group and Isc 60 min group showed behavior similar to those of iNOS; meanwhile in the Isc 90 min group, 62.5% of subjects are above TLI score 3 and in the zone of inflammatory process and irreversible damage of impedance parameters (Figure 7(c) and (d)). In the Isc 120 min group, 100% of subjects are in the zone of inflammatory process and irreversible damage. Moreover, the expression of COX-2 in all subjects of the Isc 90 and 120 min groups is in the TLI injury zone and distributed in the zone of inflammatory process and irreversible damage (Figure 7(e) and (f)).

Together, these results show that, starting from 90 min of ischemia, cells in the epithelium in the gastric mucosa significantly expressed iNOS, TNF $\alpha$ , and COX-2, biomarkers of the inflammatory process, and have apoptotic cell death in the superficial epithelium which can compromise the integrity of the epithelial barrier.

## Discussion

Shock is a pathological condition closely associated with patients with burns, acute heart failure, and brain trauma, among others. Reduced blood flow and late identification of injury in the gastrointestinal region leads to several complications associated with loss of mucosal integrity that can increase mortality in patients in critical condition.<sup>30</sup> In this work, thresholds of gastric impedance parameters are proposed to identify the time of ischemia at which the gastric mucosa is viable and maintains its barrier function. The results were confirmed with the expression analysis of iNOS, TNF $\alpha$ , COX-2, and Caspase-3, in addition to the TUNEL apoptosis assay.

The EIS allows monitoring and detection in real time of the early morphological changes that occur under conditions of oxygen deprivation.<sup>31</sup> In patients in critical condition, it is of great importance to identify early the degree of gastric mucosa injury caused by ischemia. The presence of erosions in the mucosa and dysfunction in mucus production has been identified by endoscopy by which the barrier of protection of the gastric mucosa is lost within the first 24 h of the patient's admission into intensive care. In addition, the risk of inducing splanchnic ischemia increases

with supportive interventions such as mechanical ventilation for more than 24 h and the use of vasopressors.<sup>32</sup>

In this work, early tissue changes associated with ischemia damage were detected, with an increase in low-frequency impedance parameters ( $R_L$  and  $X_L$ ); in addition, a larger increase ( $R_L$ ,  $X_L$  and  $X_H$ ) was found in the Isc 90 and Isc 120 min groups. The increase in  $R_L$  is related to edema and decreased intercellular space in narrowed joints as a result of anaerobic metabolism during ischemia. When the stimulus is much prolonged, acute adenosine triphosphate deficiency can lead to irreversible cellular damage that eventually leads to membrane destruction and cell death,<sup>33,34</sup> changes that are related to increases in reactance ( $X_L$  and  $X_H$ ).

Some papers have sought to identify tissue alterations that suggest reversible and irreversible ischemic damage and relate them to variations in impedance measurements in cardiac tissue<sup>33,34</sup> and liver.<sup>35</sup> The integrity of bowel mucosa<sup>36</sup> and intestinal viability in ischemia have been evaluated from electrical impedance measurements.<sup>30,37</sup>

Cui *et al.*<sup>35</sup> reported a gradual increase at low frequencies at 60 min of ischemia with a tendency to form a plateau after 120 min of ischemia. For their part, Strand-Amundsen *et al.*,<sup>38</sup> reported a rapid increase in  $R_L$  and  $X_H$  that are maintained during the first 3 h of ischemia before decreasing, identifying the biggest changes in  $X_H$ . Moreover,  $R_L$  has been used by Al-Surkhi and Naser<sup>39</sup> to characterize ischemic liver tissue in rabbits.

In gastric mucosa, Beltran *et al.*,<sup>18</sup> reported that  $X_L$  is the parameter best related to early damage to the gastric mucosa in patients in critical condition, in addition to proposing the  $X_L$  threshold  $>26 -j\Omega$  for patients with the greatest complications and mortality, and  $X_L <13 -j\Omega$  for patients without complications.

In the results of this work, the impedance parameters that best relate to damage to the gastric mucosa generated under prolonged ischemia conditions are  $R_L$  and  $X_H$  as reported by Strand-Amundsen *et al.*<sup>38</sup> However,  $X_L$  is a reliable indicator that allows tissue alterations to be identified early under hypoperfusion conditions.<sup>18</sup> In addition, the thresholds obtained to identify the reversibility of damage and the integrity of the gastric mucosa in the murine model are different from those proposed by Beltran *et al.*<sup>18</sup> in humans. The differences could be due to the species used in the experimental models. On the other hand, impedance values are specific to each organ, with considerable variations reported between samples of different tissues and between the same organ in different species. These variations can be caused by cytology (size, shape, and arrangement of the tissue organization of the organ), different fundamental substances and extracellular matrix (amounts of water, fat, or types of connective tissue) that essentially influence impedance at low frequencies.<sup>40</sup>

The histological results of this work show an increase in mucosal damage in a time-dependent manner. Oxygen deprivation for 60 min caused cellular lesions associated with reversible cellular damage, while starting from the Isc 90 min group, loss of intercellular and basal junctions of some epithelial cells (anoikis), in addition to increased vascular permeability (hemorrhage) was identified, culminating in the formation of ulceration zones at 120 min of

ischemia, causing the gastric mucosa to lose its barrier function. When epithelial cells are in the process of apoptosis or necrosis, substances found in the lumen may pass into the submucosa as barrier function is lost.<sup>30</sup> In the small intestine it has been identified that the epithelial lining begins to degrade after 45 min of ischemia and by increasing the duration of ischemic periods, restoration of damage induced by 120 min of reperfusion is not achieved; this results in prolonged exposure of lamina propria immune cells to molecular patterns associated with damage and pathogens.<sup>41</sup>

Magalhães *et al.*,<sup>42</sup> performed a viability analysis in rabbit stomach finding necrosis and hemorrhagic ulceration up to the muscularis propria after 3 h of ischemia. Consistent with histopathological data obtained with H&E, staining with PAS-AB showed loss of mucin secretion in the Isc 90 and Isc 120 min groups. Disruption of the mucus layer and the suppression of production can lead to an increase in epithelial permeability.<sup>43</sup> This mucus secretion coats the epithelium of the gastric mucosa protecting it from self-digestion by pepsin and acid. It has been reported that 75% of patients in critical condition present evidence of changes in mucus production within 24 h of admission to the intensive care unit.<sup>44</sup> Decreased mucin synthesis makes the gastric mucosa more susceptible to injury induced by various aggressor factors, including I/R injuries.<sup>45-47</sup> Grootjans *et al.*,<sup>46</sup> reported that the loss of the mucus barrier induced by colon ischemia for 60 min allows bacteria to penetrate and adhere to epithelial cells at both the surface and base of the crypts; therefore, early identification of ischemia in the gastrointestinal tract is critical to minimize morbidity and mortality in patients in critical condition.<sup>48</sup> iNOS is an enzyme related to the inflammatory process, which is expressed under conditions of hypoxia, and is also linked to the loss of epithelial integrity in gastric I/R models.<sup>49,50</sup> The kinetics of iNOS expression under prolonged ischemia conditions have not been reported in gastric mucosa, so it becomes important to detect the modulation of its expression in the early stages of ischemia to intervene therapeutically in order to significantly minimize the damage resulting from reperfusion. In this work, a gradual increase in the expression of iNOS in gastric epithelial cells was identified in a time-dependent manner. In *in vitro* models, Xu *et al.*,<sup>51</sup> induced the expression of iNOS by oxygen and glucose deprivation, showing an increase starting from 2 h with a maximum expression at 6 h. In addition, they identified cell death by apoptosis with an increase corresponding to the duration of deprivation. For their part, Serman *et al.*,<sup>52</sup> induced the expression of iNOS at different times of hypoxia identifying an increase after 4 h and reaching a plateau at 8 h of hypoxia. Several studies have shown that hypoxia induces the expression of iNOS, leading to rapid production of NO. In turn, NO is combined with superoxide anion to generate peroxynitrite, which causes lipoperoxidation, activation of Caspase-3 and apoptosis.<sup>53</sup>

TNF $\alpha$  is a pro-inflammatory cytokine that is induced by hypoxia and is related to increased epithelial permeability.<sup>25</sup> In this study, the expression of TNF $\alpha$  was identified in epithelial cells of the gastric mucosa at 90 min of ischemia

and descending slightly at 120 min, probably due to the degree of injury existing in the mucosa. Previous reports have identified in cardiac<sup>54</sup> and renal<sup>55</sup> cells an increase in TNF $\alpha$  levels in a time-dependent manner during oxygen deprivation. Apoptosis induced by TNF $\alpha$  alters barrier function, due to the detachment of epithelial cells which produces microerosions that cannot be sealed by redistributing proteins from narrow joints. It has been shown that epithelia can trigger extrusion after intrinsic or extrinsic apoptotic stimuli and that these extrusion pathways are partially dependent on external mitochondrial membrane permeabilization and Caspase activation.<sup>56</sup>

Since increased TNF $\alpha$  expression in plasma has been reported under conditions of gastric I/R (30 min/90 min),<sup>49</sup> in this work, iNOS and TNF $\alpha$  expressions were evaluated as tissue biomarkers of the inflammatory process in gastric mucosa. The increase of NO is related to the induction of iNOS in macrophages, neutrophils, and in affected tissues, so its elevated expression at the plasma level is more related to the inflammatory process at the systemic level and organ dysfunction.<sup>57</sup>

COX-2 is an inducible enzyme involved in inflammation and is responsible for the production of prostaglandins involved in the recovery of gastric ulcers.<sup>58,59</sup> The expression of COX-2 may be induced in response to pro-inflammatory factors (IL-1 $\alpha$ , IL-1 $\beta$ , TNF $\alpha$ , INF $\gamma$ ), with the consequent expression of COX-2 in the areas of injury, increasing the intensity of the immunohistochemical signal with the severity of tissue damage.<sup>26</sup> The results obtained in the immunohistochemical analysis are consistent with those reported, where COX-2 expression has been identified in glandular epithelium cells, surface mucous cells, mononuclear cells, fibroblasts, and endothelium in areas of injury.<sup>58</sup>

Caspase-3 immunodetection and TUNEL apoptosis assay identified the activation of Caspase-3 and the largest increase in the number of apoptotic cells in ischemic groups of 90 and 120 min, indicating the existence of irreversible biochemical processes that compromise the integrity of the gastric mucosa. Histological data and tissue damage patterns similar to those found in this work have been reported in a model of intestinal ischemia, with detachment of glandular epithelium cells after 90 min of ischemia associated with cell death by apoptosis.<sup>60</sup> Consequently, after 90 min of ischemia, apoptotic and necrotic epithelial cells could generate ulceration zones that could compromise the barrier function of the gastric mucosa.

The expression of inflammatory mediators under ischemia and I/R conditions has been studied in both males and females. It has been shown that the expression of biomarkers of the inflammatory process and apoptosis present sexual dimorphism. Female hormones affect the activation of enzymes involved in vasoregulation, including COX and iNOS, decrease TNF $\alpha$  release after intestinal ischemia, and reduce neutrophil invasion in cerebral and myocardial I/R. In addition, they exert potent antioxidant action and inhibit apoptotic pathways.<sup>61,62</sup> In an intestinal I/R model it was shown that despite transient gender-related differences in microcirculatory dysfunction, the intestinal barrier

degradation that ultimately develops after I/R is not influenced by gender.<sup>61</sup>

In conclusion, the results of this work showed morphological alterations, changes in gastric impedance and expression of markers of inflammatory process and cell death caused the gastric mucosa to lose its barrier function starting from 90 min of ischemia. It was shown that iNOS, TNF $\alpha$ , and COX-2 can be good biomarkers of damage induced by gastric ischemia. The proposed model is a good model of ischemia, which will allow future study of the therapeutic methods to reverse the damage generated at 60 min of ischemia.

#### AUTHORS' CONTRIBUTIONS

EPM, MGL and NEB designed and carried out the experiments, data acquisition, analysis, and interpretation, and wrote the manuscript. CCPM contributed with the molecular analysis and revision of the manuscript. MMA and SHY contributed with the immunohistochemical analysis, scanning and digitization for qualitative and quantitative analysis through digital pathology. All the authors read and approved the final version of the manuscript.

#### ACKNOWLEDGMENTS

This study is part of Eduardo Peña's graduate research as a doctoral student in Posgrado en Ciencias Naturales e Ingenieria, Universidad Autonoma Metropolitana - Cuajimalpa, with support from CONACYT. The authors thank the support of the Centro Nacional de Investigacion en Imagenologia e Instrumentacion Medica at the Universidad Autonoma Metropolitana-Iztapalapa, where the experiments were carried out; and the staff of the Unidad de Investigacion en Enfermedades Hematologicas, Hospital Infantil de Mexico "Federico Gomez," in particular to Daniel Hernandez-Cueto and Anahis Cruz-Ledesma for their help in processing the samples.

#### DECLARATION OF CONFLICTING INTERESTS

The author(s) declared no potential conflict of interest with respect to the research, authorship, and/or publication of this article.

#### FUNDING

The author(s) disclosed receipt of the following financial support for the research, authorship, and/or publication of this article: This work is part of Eduardo Peña-Mercado's graduate research as a doctoral student. His studies were supported from a grant from CONACYT. This research received no specific grant from any funding agency in the public, commercial, or not-for-profit sectors.

#### ORCID iDs

Peña-Mercado Eduardo  <https://orcid.org/0000-0001-7942-9624>

Beltran Nohra E  <https://orcid.org/0000-0001-7490-9127>

## REFERENCES

- Lier H, Bernhard M, Hossfeld B. Hypovolemic and hemorrhagic shock. *Anaesthesist* 2018;**67**:225–44
- Lelubre C, Vincent JL. Mechanisms and treatment of organ failure in sepsis. *Nat Rev Nephrol* 2018;**14**:417–27
- Kislitsina ON, Rich JD, Wilcox JE, Pham DT, Churyla A, Vorovich EB, Ghafourian K, Yancy CW. Shock – classification and pathophysiological principles of therapeutics. *Curr Cardiol Rev* 2019;**15**:102–13
- Beck V, Chateau D, Bryson GL, Pisipati A, Zanotti S, Parrillo JE, Kumar A. Timing of vasopressor initiation and mortality in septic shock: a cohort study. *Crit Care* 2014;**18**:1–8
- Asrani VM, Brown A, Bissett I, Windsor JA. Impact of intravenous fluids and enteral nutrition on the severity of gastrointestinal dysfunction: a systematic review and meta-analysis. *J Crit Care Med (Targu Mures)* 2020;**6**:5–24
- Pool R, Gomez H, Kellum JA. Mechanisms of organ dysfunction in sepsis. *Crit Care Clin* 2018;**34**:63–80
- Tang SJ, Daram SR, Wu R, Bhajjee F. Pathogenesis, diagnosis, and management of gastric ischemia. *Clin Gastroenterol Hepatol* 2014;**12**:246–52.e1
- Mallat J, Vallet B. Mucosal and cutaneous capnometry for the assessment of tissue hypoperfusion. *Minerva Anesthesiol* 2018;**84**:68–80
- Beltran NE, Garcia LE, Garcia-Lorenzana M. Gastric tissue damage analysis generated by ischemia: bioimpedance, confocal endomicroscopy, and light microscopy. *BioMed Res Int* 2013;**2013**:1–8
- Murdoch C, Brown BH, Hearnden V, Speight PM, D'Apice K, Hegarty AM, Tidy JA, Healey TJ, Highfield PE, Thornhill MH. Use of electrical impedance spectroscopy to detect malignant and potentially malignant oral lesions. *Int J Nanomed* 2014;**9**:4521–32
- Weijnenborg PW, Smout A, Krishnadath KK, Bergman J, Verheij J, Bredenoord AJ. Esophageal sensitivity to acid in patients with Barrett's esophagus is not related to preserved esophageal mucosal integrity. *Neurogastroenterol Motil* 2017;**29**:1–6
- Zink MD, König F, Weyer S, Willmes K, Leonhardt S, Marx N, Napp A. Segmental bioelectrical impedance spectroscopy to monitor fluid status in heart failure. *Sci Rep* 2020;**10**:1–9
- Eng CSY, Bhowruth D, Mayes M, Stronach L, Blaauw M, Barber A, Rees L, Shroff RC. Assessing the hydration status of children with chronic kidney disease and on dialysis: a comparison of techniques. *Nephrol Dial Transplant* 2018;**33**:847–55
- Kalogeris T, Baines CP, Krenz M, Korthuis RJ. Cell biology of ischemia/reperfusion injury. *Int Rev Cell Mol Biol* 2012;**298**:229–317
- Wu MY, Yang GT, Liao WT, Tsai AP, Cheng YL, Cheng PW, Li CY, Li CJ. Current mechanistic concepts in ischemia and reperfusion injury. *Cell Physiol Biochem* 2018;**46**:1650–67
- Kumar G, Kasiviswanathan U, Mukherjee S, Kumar MS, Sharma N, Patnaik R. Changes in electrolyte concentrations alter the impedance during ischemia-reperfusion injury in rat brain. *Physiol Meas* 2019;**40**:1–14
- De Ninno A, Reale R, Giovinazzo A, Bertani FR, Businaro L, Bisegna P, Matteucci C, Caselli F. High-throughput label-free characterization of viable, necrotic and apoptotic human lymphoma cells in a coplanar-electrode microfluidic impedance chip. *Biosens Bioelectron* 2020;**150**:1–8
- Beltran NE, Sanchez-Miranda G, Godinez MM, Diaz U, Sacristan E. The predictive value of gastric reactivity for postoperative morbidity and mortality in cardiac surgery patients. *Physiol Meas* 2010;**31**:1423–36
- Gezginci-Oktayoglu S, Orhan N, Bolkent S. Prostaglandin-E1 has a protective effect on renal ischemia/reperfusion-induced oxidative stress and inflammation mediated gastric damage in rats. *Int Immunopharmacol* 2016;**36**:142–50
- Peña-Mercado E, Garcia-Lorenzana M, Beltran NE. Histomorphometric analysis with a proposed tissue lesion index in ischemia-reperfusion induced gastric mucosa damage. *Histol Histopathol* 2018;**33**:1047–58
- Lee M, Wang C, Jin SW, Labrecque MP, Beischlag TV, Brockman MA, Choy JC. Expression of human inducible nitric oxide synthase in response to cytokines is regulated by hypoxia-inducible factor-1. *Free Radic Biol Med* 2019;**130**:278–87
- Yu X, Ge L, Niu L, Lian X, Ma H, Pang L. The dual role of inducible nitric oxide synthase in myocardial ischemia/reperfusion injury: friend or foe? *Oxid Med Cell Longev* 2018;**2018**:1–7
- Lima MSR, Lima VCO, Piuvezam G, Azevedo KPM, Maciel BLL, Morais AHA. Mechanisms of action of molecules with anti-TNF-alpha activity on intestinal barrier inflammation: a systematic review protocol. *Medicine (Baltimore)* 2019;**98**:1–5
- Taylor CT, Dzus AL, Colgan SP. Autocrine regulation of epithelial permeability by hypoxia: role for polarized release of tumor necrosis factor alpha. *Gastroenterology* 1998;**114**:657–68
- Bercier P, Grenier D. TNF-alpha disrupts the integrity of the porcine respiratory epithelial barrier. *Res Vet Sci* 2019;**124**:13–7
- Omayone TP, Salami AT, Olopade JO, Olaleye SB. Attenuation of ischemia-reperfusion-induced gastric ulcer by low-dose vanadium in male Wistar rats. *Life Sci* 2020;**259**:1–9
- Kamel M, Ahmed SM, Abdelzaher W. The potential protective effect of modafinil in intestinal ischemic reperfusion-induced in rats. *Int Immunopharmacol* 2020;**88**:1–8
- Wada K, Kamisaki Y, Kitano M, Kishimoto Y, Nakamoto K, Itoh T. A new gastric ulcer model induced by ischemia-reperfusion in the rat: role of leukocytes on ulceration in rat stomach. *Life Sci* 1996;**59**:PI295–301
- Beltran NE, Sacristan E. Gastrointestinal ischemia monitoring through impedance spectroscopy as a tool for the management of the critically ill. *Exp Biol Med (Maywood)* 2015;**240**:835–45
- Pan P, Song Y, Du X, Bai L, Hua X, Xiao Y, Yu X. Intestinal barrier dysfunction following traumatic brain injury. *Neurosci Lett* 2019;**40**:1105–10
- Swisher SL, Lin MC, Liao A, Leeflang EJ, Khan Y, Pavinatto FJ, Mann K, Naujokas A, Young D, Roy S, Harrison MR, Arias AC, Subramanian V, Maharbiz MM. Impedance sensing device enables early detection of pressure ulcers in vivo. *Nat Commun* 2015;**6**:1–10
- Martin B. Prevention of gastrointestinal complications in the critically ill patient. *AACN Adv Crit Care* 2007;**18**:158–66
- Schaefer M, Gross W, Gebhard MM. Hearts during ischemia with or without HTK-protection analysed by dielectric spectroscopy. *Physiol Meas* 2018;**39**:1–15
- Lueck S, Preusse CJ, Delis A, Schaefer M. Development of cell oedema in piglet hearts during ischaemia monitored by dielectric spectroscopy. *Bioelectrochemistry* 2019;**129**:54–61
- Cui ML, Ahn HS, Kim JY, Shin HJ, Lee DS, Kim HJ, Yun SS. Bioelectrical impedance may predict cell viability during ischemia and reperfusion in rat liver. *J Korean Med Sci* 2010;**25**:577–82
- Warners MJ, Vlieg-Boerstra BJ, Verheij J, van Hamersveld PHP, van Rhijn BD, Van Ampting MTJ, Harthoorn LF, de Jonge WJ, Smout A, Bredenoord AJ. Esophageal and small intestinal mucosal integrity in eosinophilic esophagitis and response to an elemental diet. *Am J Gastroenterol* 2017;**112**:1061–71
- Strand-Amundsen RJ, Tronstad C, Kalvoy H, Gundersen Y, Krohn CD, Aasen AO, Holhjem L, Reims HM, Martinsen OG, Hogetveit JO, Ruud TE, Tonnessen TI. In vivo characterization of ischemic small intestine using bioimpedance measurements. *Physiol Meas* 2016;**37**:257–75
- Strand-Amundsen RJ, Reims HM, Tronstad C, Kalvoy H, Martinsen OG, Hogetveit JO, Ruud TE, Tonnessen TI. Ischemic small intestine in vivo versus ex vivo bioimpedance measurements. *Physiol Meas* 2017;**38**:715–28
- Al-Surkhi OI, Naser RY. Detection of cell morphological changes of ischemic rabbit liver tissue using bioimpedance spectroscopy. *IEEE Trans Nanobioscience* 2018;**17**:402–8
- Bera TK. Bioelectrical impedance methods for noninvasive health monitoring: a review. *J Med Eng* 2014;**2014**:1–28
- Grootjans J, Lenaerts K, Buurman WA, Dejong CH, Derikx JP. Life and death at the mucosal-luminal interface: new perspectives on human intestinal ischemia-reperfusion. *World J Gastroenterol* 2016;**22**:2760–70
- Magalhaes MA, Barbosa AJ, Figueiredo JA, Alberti LR, Petroianu A. Effects of different periods of gastric ischaemia in the viability of the tissue of body, fundus and antrum region of rabbit stomach. *Arq Bras Cir Dig* 2015;**28**:167–70

43. Dicks LMT, Dreyer L, Smith C, van Staden AD. A review: The fate of bacteriocins in the human gastro-intestinal tract: do they cross the gut-blood barrier? *Front Microbiol* 2018;**9**:2297
44. Fennerty MB. Pathophysiology of the upper gastrointestinal tract in the critically ill patient: rationale for the therapeutic benefits of acid suppression. *Crit Care Med* 2002;**30**:S351-5
45. Mojzis J, Hegedusova R, Mirrossay L. Role of mucus in ischemia/reperfusion-induced gastric mucosal injury in rats. *Physiol Res* 2000;**49**:441-6
46. Grootjans J, Hundscheid IH, Lenaerts K, Boonen B, Renes IB, Verheyen FK, Dejong CH, von Meyenfeldt MF, Beets GL, Buurman WA. Ischaemia-induced mucus barrier loss and bacterial penetration are rapidly counteracted by increased goblet cell secretory activity in human and rat Colon. *Gut* 2013;**62**:250-8
47. Bulbul M, Tan R, Gemicci B, Ongüt G, Izgut-Uysal VN. Effect of orexin-a on ischemia-reperfusion-induced gastric damage in rats. *J Gastroenterol* 2008;**43**:202-7
48. Twhig PA, Desai A, Skeans J, Waghay N. Quantifying risk factors for ischemic colitis: a nationwide, retrospective cohort study. *Indian J Gastroenterol* 2020;**39**:398-404
49. Magierowska K, Korbut E, Hubalewska-Mazgaj M, Surmiak M, Chmura A, Bakalarz D, Buszewicz G, Wojcik D, Sliwowski Z, Ginter G, Gromowski T, Kwiecien S, Brzozowski T, Magierowski M. Oxidative gastric mucosal damage induced by ischemia/reperfusion and the mechanisms of its prevention by carbon monoxide-releasing tricarbonyldichlororuthenium (II) dimer. *Free Radic Biol Med* 2019;**145**:198-208
50. Peña-Mercado E, Garcia-Lorenzana M, Arechaga-Ocampo E, González-De la RC, Beltran NE. Evaluation of HIF-1 $\alpha$  and iNOS in ischemia/reperfusion gastric model: bioimpedance, histological and immunohistochemical analyses. *Histol Histopathol* 2018;**33**:815-23
51. Xu J, He L, Ahmed SH, Chen SW, Goldberg MP, Beckman JS, Hsu CY. Oxygen-glucose deprivation induces inducible nitric oxide synthase and nitrotyrosine expression in cerebral endothelial cells. *Stroke* 2000;**31**:1744-51
52. Serman Y, Fuentealba RA, Pasten C, Rocco J, Ko BCB, Carrion F, Irrarrazabal CE. Emerging new role of NFAT5 in inducible nitric oxide synthase in response to hypoxia in mouse embryonic fibroblast cells. *Am J Physiol Cell Physiol* 2019;**317**:C31-C38
53. Guo M, Ma X, Feng Y, Han S, Dong Q, Cui M, Zhao Y. In chronic hypoxia, glucose availability and hypoxic severity dictate the balance between HIF-1 and HIF-2 in astrocytes. *FASEB J* 2019;**33**:11123-36
54. Yu X, Deng L, Wang D, Li N, Chen X, Cheng X, Yuan J, Gao X, Liao M, Wang M, Liao Y. Mechanism of TNF-alpha autocrine effects in hypoxic cardiomyocytes: initiated by hypoxia inducible factor 1alpha, presented by exosomes. *J Mol Cell Cardiol* 2012;**53**:848-57
55. Meldrum KK, Meldrum DR, Hile KL, Yerkes EB, Ayala A, Cain MP, Rink RC, Casale AJ, Kaefer MA. p38 MAPK mediates renal tubular cell TNF-alpha production and TNF-alpha-dependent apoptosis during simulated ischemia. *Am J Physiol Cell Physiol* 2001;**281**:C563-70
56. Watson AJ, Hughes KR. TNF-alpha-induced intestinal epithelial cell shedding: implications for intestinal barrier function. *Ann N Y Acad Sci* 2012;**1258**:1-8
57. Kumar S, Gupta E, Srivastava VK, Kaushik S, Saxena J, Goyal LK, Mehta S, Jyoti A. Nitrosative stress and cytokines are linked with the severity of sepsis and organ dysfunction. *Br J Biomed Sci* 2019;**76**:29-34
58. Mahmoud YI, Abd El-Ghffar EA. Spirulina ameliorates aspirin-induced gastric ulcer in albino mice by alleviating oxidative stress and inflammation. *Biomed Pharmacother* 2019;**109**:314-21
59. Fagundes FL, de Moraes Piffer G, Perico LL, Rodrigues VP, Hiruma-Lima CA, Dos SR. Chrysin modulates genes related to inflammation, tissue remodeling, and cell proliferation in the gastric ulcer healing. *Int J Mol Sci* 2020;**21**:1-12
60. Ikeda H, Suzuki Y, Suzuki M, Koike M, Tamura J, Tong J, Nomura M, Itoh G. Apoptosis is a major mode of cell death caused by ischaemia and ischaemia/reperfusion injury to the rat intestinal epithelium. *Gut* 1998;**42**:530-7
61. Szabó A, Vollmar B, Boros M, Menger MD. Gender differences in ischemia-reperfusion-induced microcirculatory and epithelial dysfunctions in the small intestine. *Life Sci* 2006;**78**:3058-65
62. Liu F, Li Z, Li J, Siegel C, Yuan R, McCullough LD. Sex differences in caspase activation after stroke. *Stroke* 2009;**40**:1842-8

(Received January 21, 2021, Accepted May 13, 2021)